[Global Biogeochemical Cycles]

Supporting Information for

Identifying the most (cost-)efficient regions for CO_2 removal with Iron Fertilization in the Southern Ocean

Lennart T. Bach[1]*, Veronica Tamsitt[2], Kimberlee Baldry[1], Jeffrey McGee[1,3], Emmanuel C. Laurenceau-Cornec[1,4], Robert F. Strzepek[1,5], Yinghuan Xie[1], Philip W. Boyd[1,5]

[1]Institute for Marine and Antarctic Studies, University of Tasmania, Hobart, Tasmania, Australia.

[2]College of Marine Science, University of South Florida, St Petersberg, Florida, USA.

[3]Faculty of Law, University of Tasmania, Hobart, Tasmania, Australia.

[4]Univ. Brest, CNRS, IRD, Ifremer, LEMAR, Plouzane, France.

[5]Australian Antarctic Program Partnership, Hobart, Tasmania, Australia.

Contents of this file

Introduction

The supporting information file contains more detailed method descriptions (Text S1-S3), figures (S1-S4) and tables (S1-S6) ordered as they occur in the main text of the paper and the supplement. Figures and tables provide more detailed aspects of certain parts of the analysis. Text S1 provides mathematical details of estimating limitations on OIF (cost-)efficiency set by air-sea CO_2 exchange. Text S2 provides details on estimates of DFe limitation in natural phytoplankton communities, while Text S3 provides details on estimating light limitation.

Text S1

In the OIF scenario, the DIC perturbation (DIC_{ptb}) cumulatively changes along a particle trajectory according to the amount of DIC that has been added to the system by air-sea gas exchange and always exhibits a CO_2 influx relative to the no-OIF scenario (i.e. the background biogeochemical state; Fig. S1A). This is represented as:

$$DIC_{ptb}\ (t > 0) = 35 - \sum_{t=0}^{n-1} \times (\Delta DIC'(t) - \Delta DIC(t)) \quad (1)$$

where DIC_{ptb}(t=0) is 35 µmol kg^{-1}, **Δ**DIC(t) is the DIC added to the system over 5 days due to air-sea gas exchange of the expected biogeochemical state at timestep t, and **Δ**DIC'(t) is the DIC added to the system over 5 days due to air-sea gas exchange of the perturbed system at timestep t.
To derive DIC_{ptb}, consider the derivation of ***Δ***DIC from air-sea fluxes for the no-OIF and the OIF scenarios. ***Δ***DIC is calculated by first calculating air-sea CO_2 flux (F) over the mixed layer.

$$F = G \times K_0 \times (pCO_{2\_SW} - pCO_{2\_air}) \quad (2)$$

where G is the gas-exchange constant (m s^{-1}), K_0 is the solubility constant (mol m^{-3} atm^{-1}), pCO_{2_SW} is the partial pressure of CO_2 in seawater (µatm) and pCO_{2_air} is the partial pressure of CO_2 in air (µatm). Then ***Δ***DIC (µmol kg^{-1}) can subsequently calculated by iteratively integrating F over 5 days

$$\Delta DIC = \frac{F \times t}{h \times \rho} \quad (3)$$

where t is 5 days (s), ***ρ*** is the density of seawater (kg m^{-3}) calculated from salinity and temperature using seacarb (Gattuso et al. 2021), h is the mixed-layer depth (m) from MOM01.
Thus to calculate DIC*_ptb*, equation (1) should be expanded using equations (2) and (3) with the assumption that atmospheric pCO_2 remains unchanged between the two scenarios.

$$DIC_{ptb}(t > 0) = 35 + \sum_{t=0}^{n-1} \frac{G(t) \times K_0 \times t}{h(t) \times \rho(t)} (pCO'_{2\_SW}(t) - pCO_{2\_SW}(t)) \quad (4)$$

The gas exchange constant (G) was calculated using daily mean climatologies of wind speed, temperature and salinity (Table S3) according to Wanninkhof (2014). We linearly scaled G to sea-ice concentration (Butterworth and Miller 2016; Prytherch et al. 2017). The solubility constant (K_0) was calculated using the fourth order polynomial of Wanninkhof (2014). MOM01 model mixed layer depth (h) and the density of seawater (ρ) was calculated from salinity and temperature (Table S3) using the function "rho" from the R "seacarb" package (Gattuso et al. 2021).
To calculate $pCO'_{2\_SW}(t)$ and the carbonate system at the alternate state, we calculated perturbed DIC (DIC'(t)) at each time step using the expected DIC from the no-OIF scenario (DIC(t)) and the amount of DIC added by air-sea gas exchange due to the OIF deficit (DIC_{ptb}):

$$DIC'(t) = DIC(t) - DIC_{ptb}(t) \quad (5)$$

where DIC(t) was calculated from 1x1 monthly mean climatologies and modeled alkalinity (from the Locally Interpolated Alkalinity Regression v2, (Carter et al. 2018)) using the "carb" function in the R package "seacarb" (Gattuso et al. 2021) with K1 and K2 constants from Millero et al. (2006). DIC'(t) was then used to calculate the perturbed pCO_2 of the seawater pCO_2'$_{SW}$ at each time-step (Millero et al. 2006; Gattuso et al. 2021). We assumed that alkalinity changes are negligible.
Finally, we can calculate the fraction of the DIC deficit that is replenished by atmospheric CO_2 influx (f_{Eq}) at each time-step:

$$f_{Eq} = \left(\frac{1 - DIC_{ptb}}{35}\right) \quad (6)$$

We only calculated f_{Eq} where sea-ice concentration was <60%. This minimized the amount of missing data within our calculations and allowed more trajectories to be included in our analysis, but underestimates CO_2 in-gassing over time under sea-ice, as gas exchange is expected to vary linearly with sea-ice concentration (Butterworth and Miller 2016; Prytherch et al. 2017). The OIF scenario was considered fully equilibrated when $DIC_{ptb} \leq 0$, converging to the no-OIF scenario (Fig. S1B).

Text S2

We synthesized published shipboard iron-amendment experiments using the following search query on Google Scholar (31, July 2019): "phytoplankton" OR "microalgae" OR "algae" OR "diatom" OR "Phaeocystis" AND "iron" AND "growth" AND "Southern Ocean" OR "Antarctic" OR "Antarctica". The first 200 hits were inspected. Relevant datasets were those where natural communities from south of the polar front were incubated under iron-replete (+Fe) and iron-deplete (-Fe) conditions and growth rates from both treatments, as well as background dissolved iron (DFe) concentrations were reported (Table S1). An additional search with the same query but restricting the search to papers published since 2015 was done afterwards because there was a bias towards older and more frequently cited literature.
Growth rates (μ) were calculated from chlorophyll a (chla) increase, particulate organic carbon (POC) accumulation, or nitrate draw-down. In some studies growth rates were not provided as numbers but had to be calculated using the following equation:

$$\mu = \frac{ln\,(t_{end}) - ln\,(t_{start})}{d} \qquad (7)$$

where t_{start} and t_{end} is chla or POC concentration at the start and the end of the experiment, respectively and d is the duration of the experiment in days. (Please note that it was $ln(t_{start})$-$ln(t_{end})$ in the numerator of equation 7 in calculations using nitrate drawdown.). For this calculation, data often (especially in the older literature) needed to be extracted from plots using the data grabbing tool WebPlotDigitizer (https://automeris.io/WebPlotDigitizer/). We calculated the fold change of growth rate and plotted μ_{+Fe}/μ_{-Fe} as a function of the *in situ* background (i.e. pre-treatment) DFe concentration from the batch of seawater which was incubated. Bioavailability of DFe was not considered as this was seldom reported in the literature.

Text S3

We applied the observation-based approach of Venables and Moore (2010) to assess if light could limit phytoplankton growth during summer south of 60°S. Satellite and Argo float data were used to calculate the mean irradiance in the surface mixed layer (I_{MLD}) and compare this to the threshold irradiance above which phytoplankton communities can grow (I_{MLD_min}).
I_{MLD} (mol photons m^{-2} d^{-1}) was calculated as:

$$I_{MLD} = \frac{PAR_{belowsurf}}{K_d h}(1 - e^{-K_d h}) \qquad (8)$$

where $PAR_{belowsurf}$ is the photosynthetically active radiation (PAR) just below the sea surface (mol photons m^{-2} d^{-1}), K_d the diffuse downwelling attenuation coefficient (m^{-1}), and h the mixed layer depth (m). Downwelling $PAR_{belowsurf}$ is lower than PAR above the surface ($PAR_{abovesurf}$) because part of the sunlight is reflected at the sea surface. The reflected fraction at the air-sea interface depends on a range of factors such as sun zenith angle, wind speed, or cloud cover (Campbell and Aarup 1989; Mobley and Boss 2012). Between 60 – 70°S, reflection is approximately 7% for clear sky conditions and calm water during summer (less reflection for wind speed >0 m/s and overcast sky (Campbell and Aarup 1989; Mobley and Boss 2012). Sea ice is another medium that absorbs light before it can enter the ocean. Light absorption by sea ice depends on snow cover or the presence of melt ponds on ice but was shown to be on average 0.957 (mean transmission = 0.043) (Katlein et al. 2019). Using this information, we approximated $PAR_{belowsurf}$ as:

$$PAR_{belowsurf} = PAR_{abovesurf} * (0.07 * IC + 0.93) * (1 - IC * 0.957) \qquad (9)$$

where IC is the sea ice cover from 0 (no ice) to 1 (complete coverage). This equation balances the influence of reflection of PAR at the liquid air-sea interface and the absorption of PAR by sea ice within a grid field. K_d was estimated from satellite chlorophyll a following (Venables and Moore 2010):

$$K_d = 0.05 + 0.057 * chla^{0.58} \quad (10)$$

where chla is the chlorophyll a concentration in mg m^{-3}. $PAR_{abovesurf}$, IC, and chla were obtained from the NASA Giovanni online data system. More specifically, we downloaded gridded data of austral summer averages (December-February (DJF) 2010-2020) of "photosynthetically available radiation (MODISA_L3m_PAR v2018)" and "Sea-ice covered fraction of tile (M2TMNXFLX v5.12.4)" from the MERRA-2 Model, and "Chlorophyll a concentration (MODISA_L3m_CHL v2018)" from the MERRA-2 Model.

We used an Argo-based climatology to obtain mean DJF mixed layer depths (h) for south of 60°S (Holte et al. 2017). Spatial resolution differed between $PAR_{abovesurf}$, chla (both 1/24 degree), IC (0.5 x 0.625 (lat x lon) degree), and h (0.5 degree), so that they were re-gridded to 0.5 degrees using raster functions and bilinear interpolation with the software R. Mixed layer depth, as well as K_d, IC, and $PAR_{belowsurf}$ are shown in Fig. S2.

Venables and Moore (2010) determined an I_{MLD_min} of 3 mol photons m^{-2} d^{-1} in the Southern Ocean by comparing I_{MLD} in Fe-limited regions with I_{MLD} in naturally Fe-fertilized regions (e.g. near the Kerguelen Islands). To further constrain I_{MLD_min}, we explored the literature for growth vs. irradiance curves with Southern Ocean phytoplankton species. Our goal was to approximate the daily irradiance above which growth rates are saturated. The reason why we specifically looked for growth rates and not photosynthesis rates is that growth rates are measured over days to weeks while photosynthesis rates are usually measured for hours. Thus, phytoplankton can be assumed to be acclimated to the light levels they are exposed to during the incubation. To find relevant studies we used Google Scholar (29 April 2020) and searched for: "Light" OR "Irradiance" OR "radiation" AND "Southern Ocean" AND "phytoplankton". We only found 2 relevant studies in the first 100 hits so we looked more specifically into the reference lists of these 2 studies and found another 2. We normalized growth rates at each light level to the maximum growth rate measured within a growth vs. irradiance curve (Table S2). Finally, we fitted a growth vs. irradiance model (Eilers and Peeters 1988) to the binned data to determine the irradiance that corresponds to the onset of irradiance saturation. The data also suggest the potential for light inhibition at high irradiance but this aspect is not considered in our study as it may reduce growth rates but is unlikely to stop growth (i.e. growth rates remained positive in the data compiled at high irradiance).

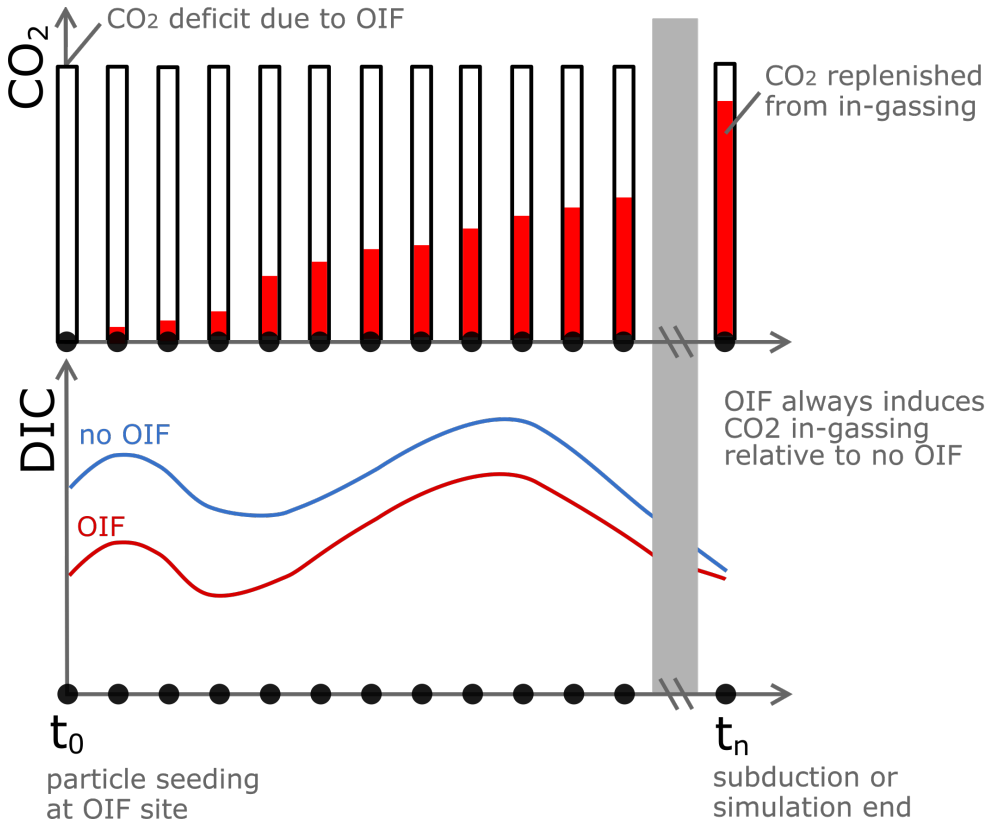

Fig S1. Conceptual framework of the air-sea CO_2 equilibration calculation. (**A**) Representation of the "bucket" approach. The initial DIC deficit (equivalent to a seawater CO_2 deficit) of 35 µmol/kg gradually (white bar) fills up with atmospheric CO_2 (red bar) over time until the water parcel carrying the deficit subducts below the mixed layer. The extent to which the bucket is full at the time of exiting the mixed layer (f_{Eq}) is the target variable of this calculation. (**B**) Representation of the background biogeochemical state of DIC (no OIF scenario; blue line) and how a hypothetical OIF operation which generated a 35 µmol/kg DIC deficit (red line) approaches the background state over time through atmospheric CO_2 influx. Strengths and weaknesses of this approach are discussed in section 3.1.5.

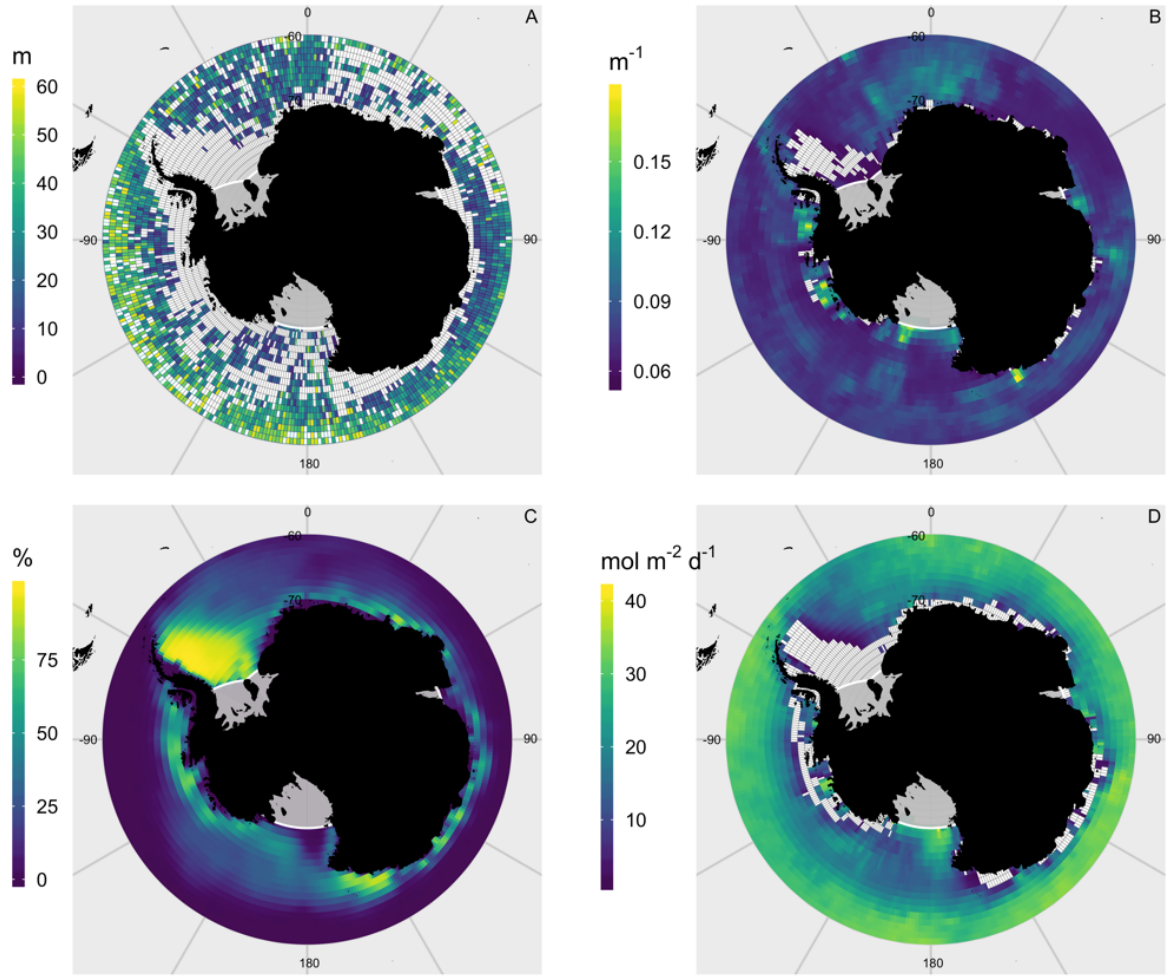

Fig. S2. The four parameters used to calculate austral summer (December-February) I_{MLD}. (A) Mixed layer depth (h). The attenuation of PAR (K_d). (C) Ice cover (IC). (D) Incoming photosynthetically available radiation just below the sea surface ($PAR_{belowsurf}$).

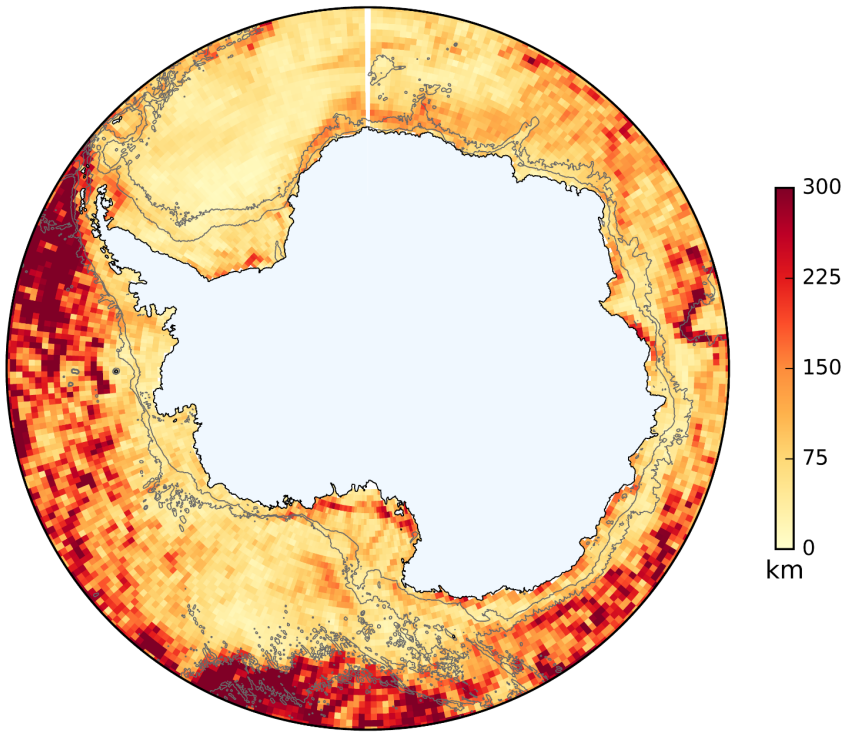

Fig. S3. Mean net distance neutrally-buoyant particles seeded in January drift horizontally within 1 month from release. Particles are binned in 0.5° latitude by 1° longitude bins by starting location and the color indicates the average distance traveled (net horizontal distance in km) from the starting location of all particles released within each bin. Distances are large in the Antarctic Circumpolar Current (ACC) but generally shorter in the Weddell and Ross Gyres and coastal areas, except for some faster coastal currents.

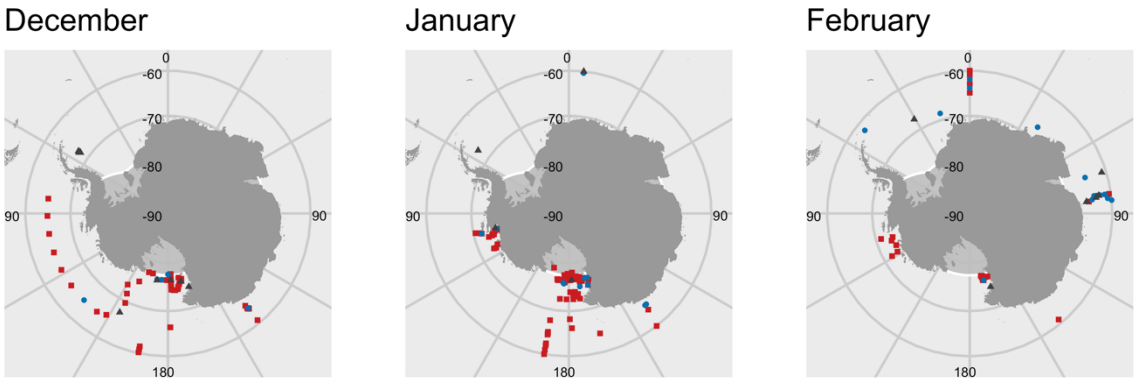

Fig. S4. Monthly surface (0-100 m) DFe surface concentrations. Red squares = 0 – 0.25 = "limited"; Blue circles = >0.25 – 0.5 nM = "mildly-limited"; Grey pyramids = >0.5 = non-limited).

Table S1. Summary of the literature analysis to constrain the onset of Iron limitation. Lon. is longitude. Lat. is latitude. Depth is the depth from where the incubated communities were collected (in m). DoE are the days of experiment. V. is the incubation volume (in L). Incub. indicates whether communities were incubated on the deck of a research vessel or in its laboratories. PAR is the photosynthetically active radiation the communities were exposed to during the experiments. Numbers are either given in µmol m^{-2} s^{-1} or as percentage of ambient light provided. L:D is the light/dark cycle (hour:hour) during a day. Ambient indicates an L:D cycle at the position of the research vessel during the experiment. T is the incubation temperature in °C. Ambient indicates a temperature at the position of the research vessel during the experiment. DFe, N, P, and Si are the background concentrations of dissolved iron, nitrate, phosphate, and silicate, in the batch of the incubated water when it was collected. Meth. indicates how growth rates were measured (chla = increase of chlorophyll a concentration; POC = increase of particulate organic carbon concentrations; NO3 = decrease of nitrate concentrations). μ_{+Fe} are the community growth rates in the +Fe treatment. μ_{-Fe} are the community growth rates in the un-amended controls. μ_{+Fe}/μ_{-Fe} is the fold-change in community growth rates due to Fe enrichment.

Reference	Lon.	Lat.	Depth	DoE	V.	Incub.	PAR	L:D	T	DFe	N	P	Si	Meth.	μ_{+Fe}	μ_{-Fe}	μ_{+Fe}/μ_{-Fe}
(Coale et al. 2003)	178.00	-76.50	25	8	20	Deck	120 %	amb.	amb.	0.03	21.6	1.64	71	chla[a]	0.230	0.137	1.683
(Coale et al. 2003)	176.00	-74.30	25	13	20	Deck	120 %	amb.	amb.	0.04	26.9	1.9	63.5	chla[a]	0.207	0.096	2.153
(Coale et al. 2003)	170.00	-62.30	50	18	20	Deck	120 %	amb.	amb.	0.1	31.1	2.06	45.9	chla[a]	0.250	0.146	1.717
(Coale et al. 2003)	170.00	-59.30	50	16	20	Deck	120 %	amb.	amb.	0.06	26.8	1.83	15.2	chla[a]	0.110	0.053	2.065
(Coale et al. 2003)	170.10	-67.80	20	15	20	Deck	120 %	amb.	amb.	<0.03	25.1	1.56	59.8	chla[a]	0.260	0.071	3.646
(Coale et al. 2003)	170.10	-62.00	25	16	20	Deck	120 %	amb.	amb.	0.11	22.6	1.43	4.9	chla[a]	0.120	0.036	3.337
(Bertrand et al. 2007)	-179.38	-74.43	5-8	6	1.1	Deck	20%	amb.	amb.	0.31	19.89	1.36	63.64	chla[b]	0.228	0.110	2.077
(Bertrand et al. 2007)	179.11	-76.00	5-8	9	1.1	Deck	20%	amb.	amb.	0.11	20	1.33	62	chla[c]	0.254	0.095	2.686
(Bertrand et al. 2007)	173.30	-75.00	5-8	8	1.1	Deck	20%	amb.	amb.	0.13	22.98	1.63	62	chla[c]	0.465	0.215	2.165

(Bertrand et al. 2007)	168.96	-76.65	10	7	0.06	Deck	20%	amb.	amb.	0.09	13.37	1.49	74.75	chla[c]	0.360	0.240	1.500
(Takeda 1998)	140.70	-64.20	10-15	7	12	Deck	40%	amb.	amb.	0.16	22.8	1.24	18.7	chla	0.430	0.130	3.308
(Takeda 1998)	140.70	-64.20	10-15	7	12	Deck	2.60%	amb.	amb.	0.16	22.8	1.24	18.7	chla	0.400	0.130	3.077
(Cullen et al. 2003)	-170.10	-67.80	20	10.7	20	Deck	120%	amb.	amb.	0.03	25.1	1.54	60	chla	0.280	0.150	1.867
(Öztürk et al. 2004)	6.00	-56.5	15	13	12	Deck	50%	amb.	amb.	0.47	29		60	chla	0.323	0.236	1.368
(Sedwick et al. 2000)	179.95	-76.48	0.3	6	1.2	Deck	50%	amb.	amb.	0.82	27.5			chla[b]	0.167	0.306	0.545
(Sedwick et al. 2000)	170.73	-76.50	0.4	7	2.2	Deck	50%	amb.	amb.	2.2	26			chla[b]	0.335	0.335	1.000
(Van Leeuwe et al. 1997)	-6.20	-57.3			20	Lab	100	16:8	1	0.6	repl.	repl.	repl.	chla[d]	0.197	0.230	0.857
(Van Leeuwe et al. 1997)	-6.00	-48.82			20	Lab	100	16:8	1	0.5	repl.	repl.	repl.	chla[d]	0.280	0.215	1.302
(Van Leeuwe et al. 1997)	-6.00	-47			20	Lab	100	16:8	1	3.5	23	1.6	14	chla[d]	0.450	0.350	1.286
(Van Leeuwe et al. 1997)	-6.27	-59			20	Lab	100	16:8	1	0.5	repl.	repl.	repl.	chla[d]	0.385	0.345	1.116
(Sedwick et al. 2007)	173.23	-73.4	0.3		1	Deck	15%	amb.	0	0.38	20	1.5	55	chla[c]	0.390	0.386	1.008
(Sedwick et al. 2007)	173.23	-73.4	0.3		1	Deck	15%	amb.	0	0.38	20	1.5	55	chla[c]	0.210	0.179	1.169

(Timmermans et al. 1998)	-91.83	-67.21	40	3	20	Lab	80	8:16	3.5	0.31	24.72	1.73	14.22	chla	0.003	0.005	0.531
(Rose et al. 2009)	177.36	-75	surface		4.5	Deck	18%	amb.	0	0.15	25.8	1.9	68	chla	0.296	0.142	2.087
(Kustka et al. 2015)	178.00	-74.5	33-44	10	8	Lab	40	24:0	1.5	0.235	18.6		56.9	chla	0.258	0.099	2.606
(Kustka et al. 2015)	178.50	-72.58	25-35	9	8	Lab	40	24:0	1.5	0.188	27.7		58.5	chla	0.242	0.118	2.051
(Kustka et al. 2015)	176.65	-74.14	30-40	9	8	Lab	40	24:0	1.5	0.12	27.6		66	chla	0.262	0.105	2.495
(Kustka et al. 2015)	178.75	-74.20	25-35		8	Lab	40	24:0	1.5	0.127	22.4		61.4	chla	0.365	0.160	2.281
(Hopkinson et al. 2007)	-57.70	-60.5	20	7-14	4	Lab	218	24:0	2.5	0.14				chla	0.320	0.150	2.133
(Hopkinson et al. 2007)	-57.70	-60.5	85	7-14	4	Lab	37	24:0	2.5	0.12				chla	0.340	0.140	2.429
(Hopkinson et al. 2007)	-54.10	-59.6	25	7-14	50	Lab	185	24:0	2.5	0.09				chla	0.240	0.110	2.182
(Hopkinson et al. 2007)	-54.90	-59.4	20	11	4	Lab	139	24:0	2.5	0.11	22			chla	0.230	0.080	2.875
(Hopkinson et al. 2007)	-54.90	-59.4	50	7-14	4	Lab	34	24:0	2.5	0.31				chla	0.340	0.170	2.000
(Hopkinson et al. 2007)	-58.00	-61.2	20	7-14	4	Lab	218	24:0	2.5	1.74				chla	0.210	0.190	1.105
(Hopkinson et al. 2007)	-54.40	-60.9	20	14	4	Lab	218	24:0	2.5	1.59	28			chla	0.420	0.370	1.135
(Viljoen et al. 2018)	0.00	-65	30		2.4	Lab	25	amb.	0	0.19	25.2		74.3	chla[e]	0.230	0.130	1.769

(Viljoen et al. 2018)	0.00	-65	30		2.4	Lab	65	amb.	0	0.19	25.2		74.3	chla[e]	0.260	0.150	1.733
(Wu et al. 2019)	166.67	-77.85		7	0.3	Lab	80	24:0	0.5	1.01				chla	0.221	0.126	1.752
(Wu et al. 2019)	166.67	-77.85		8	0.3	Lab	80	24:0	0.5	0.47				chla	0.172	0.190	0.903
(Alderkamp et al. 2019)	177.51	-77	10.2	6	2	Deck	3%	amb.	-0.5	0.086	20.3	1.45	71.7	POC	0.180	0.124	1.452
(Alderkamp et al. 2019)	177.51	-77	10.2	6	2	Deck	30%	amb.	-0.5	0.086	20.3	1.45	71.7	POC	0.225	0.169	1.331
(Alderkamp et al. 2019)	177.50	-77.32	9.97	6	2	Deck	3%	amb.	-0.5	0.067	23.2	1.61	70.8	POC	0.208	0.141	1.475
(Alderkamp et al. 2019)	177.50	-77.32	9.97	6	2	Deck	30%	amb.	-0.5	0.067	23.2	1.61	70.8	POC	0.245	0.168	1.458
(Alderkamp et al. 2019)	171.00	-77	25.01	6	2	Deck	3%	amb.	-0.5	0.09	21.7	1.53	70.1	POC	0.120	0.092	1.304
(Alderkamp et al. 2019)	171.00	-77	25.01	6	2	Deck	30%	amb.	-0.5	0.09	21.7	1.53	70.1	POC	0.206	0.159	1.296
(Alderkamp et al. 2019)	171.00	-76.5	23.5	6	2	Deck	3%	amb.	-0.5	0.061	17.7	1.06	57.4	POC	0.067	0.024	2.792
(Alderkamp et al. 2019)	171.00	-76.5	23.5	6	2	Deck	30%	amb.	-0.5	0.061	17.7	1.06	57.4	POC	0.156	0.091	1.714
(Alderkamp et al. 2019)	10.03	-53.01	24	10-15	4	Lab	30	24:0	3	0.23	24.6	1.6	32.1	NO3[f]	0.052	0.031	1.692
(Endo et al. 2017)	140.05	-59	15	3.3	9	Lab	100	17:7	3.6	0.043	24.96	1.59	11.11	chla	0.351	0.103	3.400

(Endo et al. 2017)	110.00	-60	15	3.7	9	Lab	100	18.5:5.5	2.5	0.052	25.82	1.61	29.54	chla	0.405	0.084	4.816
(Endo et al. 2017)	138.08	-60.35	15	4	9	Lab	100	19.25:4.75	1	0.024	25.7	1.65	39.75	chla	0.482	0.462	1.042

[a]data extracted from plots except for the control.
[b]data extracted from plots. t_{end} was the value before N, P, or Si were limiting.
[c]data extracted from plots.
[d]the authors excluded the lag phase that occurred directly after the Fe addition
[e]the authors also measured POC based growth and these values were different to the chla based values. We chose their chla based values for consistency with most other datasets.
[f]the authors diluted the experiment multiple times. We used only values before the first dilution.

Table S2. Summary of the literature analysis for growth vs. irradiance curve of Southern Ocean phytoplankton. I is the growth irradiance in µmol m^{-2} s^{-1}. L:D is the light:dark cycle of the incubation in hour:hour. PAR is the photosynthetically active radiation the communities were exposed to in mol m^{-2} d^{-1}. T is the incubation temperature in °C. Ambient indicates a temperature at the position of the research vessel during the experiment. N, P, and Si are the concentrations of dissolved nitrate, phosphate, and silicate during incubations. Rel. µ is the growth rate normalized to the maximum growth rate observed in a growth vs. irradiance curve. Exp. indicates that data belongs to the same growth vs. irradiance curve.

Authors	I	L:D	PAR	T	N	P	Si	Species	Rel. µ	Exp
(Strzepek et al. 2012)	570	24:0	49.2	3.0	300	10	100	*Phaeocystis antarctica*	0.82	1
(Strzepek et al. 2012)	400	24:0	34.6	3.0	300	10	100	*Phaeocystis antarctica*	1.00	1
(Strzepek et al. 2012)	98	24:0	8.5	3.0	300	10	100	*Phaeocystis antarctica*	0.61	1
(Strzepek et al. 2012)	57	24:0	4.9	3.0	300	10	100	*Phaeocystis antarctica*	0.64	1
(Strzepek et al. 2012)	34	24:0	2.9	3.0	300	10	100	*Phaeocystis antarctica*	0.45	1
(Strzepek et al. 2012)	18	24:0	1.6	3.0	300	10	100	*Phaeocystis antarctica*	0.42	1
(Strzepek et al. 2012)	8	24:0	0.7	3.0	300	10	100	*Phaeocystis antarctica*	0.21	1
(Strzepek et al. 2012)	3	24:0	0.3	3.0	300	10	100	*Phaeocystis antarctica*	0.15	1
(Strzepek et al. 2012)	100	24:0	8.6	3.0	300	10	100	*Phaeocystis antarctica*	1.00	2
(Strzepek et al. 2012)	70	24:0	6.0	3.0	300	10	100	*Phaeocystis antarctica*	0.97	2
(Strzepek et al. 2012)	30	24:0	2.6	3.0	300	10	100	*Phaeocystis antarctica*	0.91	2
(Strzepek et al. 2012)	10	24:0	0.9	3.0	300	10	100	*Phaeocystis antarctica*	0.67	2
(Strzepek et al. 2012)	3	24:0	0.3	3.0	300	10	100	*Phaeocystis antarctica*	0.47	2

(Strzepek et al. 2012)	100	24:0	8.6	3.0	300	10	100	*Proboscia inermis*	1.00	3
(Strzepek et al. 2012)	70	24:0	6.0	3.0	300	10	100	*Proboscia inermis*	0.92	3
(Strzepek et al. 2012)	30	24:0	2.6	3.0	300	10	100	*Proboscia inermis*	0.75	3
(Strzepek et al. 2012)	10	24:0	0.9	3.0	300	10	100	*Proboscia inermis*	0.44	3
(Strzepek et al. 2012)	3	24:0	0.3	3.0	300	10	100	*Proboscia inermis*	0.22	3
(Strzepek et al. 2012)	100	24:0	8.6	3.0	300	10	100	*Eucampia antarctica*	1.00	4
(Strzepek et al. 2012)	70	24:0	6.0	3.0	300	10	100	*Eucampia antarctica*	1.00	4
(Strzepek et al. 2012)	30	24:0	2.6	3.0	300	10	100	*Eucampia antarctica*	0.72	4
(Strzepek et al. 2012)	10	24:0	0.9	3.0	300	10	100	*Eucampia antarctica*	0.74	4
(Strzepek et al. 2012)	3	24:0	0.3	3.0	300	10	100	*Eucampia antarctica*	0.55	4
(Arrigo et al. 2010)	5	24:0	0.4	2.0	300	10	repl.	*Fragilariopsis cylindrus*	0.55	5
(Arrigo et al. 2010)	25	24:0	2.2	2.0	300	10	repl.	*Fragilariopsis cylindrus*	0.91	5
(Arrigo et al. 2010)	65	24:0	5.6	2.0	300	10	repl.	*Fragilariopsis cylindrus*	1.00	5
(Arrigo et al. 2010)	125	24:0	10.8	2.0	300	10	repl.	*Fragilariopsis cylindrus*	0.82	5
(Arrigo et al. 2010)	5	24:0	0.4	2.0	300	10		*Phaeocystis antarctica*	0.26	6
(Arrigo et al. 2010)	25	24:0	2.2	2.0	300	10		*Phaeocystis antarctica*	0.86	6
(Arrigo et al. 2010)	65	24:0	5.6	2.0	300	10		*Phaeocystis antarctica*	1.00	6
(Arrigo et al. 2010)	125	24:0	10.8	2.0	300	10		*Phaeocystis antarctica*	0.63	6
(Arrigo et al. 2010)	5	24:0	0.4	2.0	300	10		*Phaeocystis antarctica*	0.20	7
(Arrigo et al. 2010)	25	24:0	2.2	2.0	300	10		*Phaeocystis antarctica*	0.34	7

(Arrigo et al. 2010)	65	24:0	5.6	2.0	300	10		*Phaeocystis antarctica*	0.71	7
(Arrigo et al. 2010)	125	24:0	10.8	2.0	300	10		*Phaeocystis antarctica*	0.63	7
(Timmermans et al. 2007)	15	16:8	0.8	4.0	80	5	80	*Chaetoceros brevis*	0.00	8
(Timmermans et al. 2007)	18	16:8	1.0	4.0	80	5	80	*Chaetoceros brevis*	0.58	8
(Timmermans et al. 2007)	38	16:8	2.2	4.0	80	5	80	*Chaetoceros brevis*	0.71	8
(Timmermans et al. 2007)	45	16:8	2.6	4.0	80	5	80	*Chaetoceros brevis*	0.86	8
(Timmermans et al. 2007)	65	16:8	3.7	4.0	80	5	80	*Chaetoceros brevis*	0.91	8
(Timmermans et al. 2007)	78	16:8	4.5	4.0	80	5	80	*Chaetoceros brevis*	0.92	8
(Timmermans et al. 2007)	100	16:8	5.7	4.0	80	5	80	*Chaetoceros brevis*	1.00	8
(Timmermans et al. 2007)	12	16:8	0.7	4.0	80	5	80	*Thalassiosira antarctica*	0.01	9
(Timmermans et al. 2007)	14	16:8	0.8	4.0	80	5	80	*Thalassiosira antarctica*	0.53	9
(Timmermans et al. 2007)	30	16:8	1.7	4.0	80	5	80	*Thalassiosira antarctica*	0.68	9
(Timmermans et al. 2007)	40	16:8	2.3	4.0	80	5	80	*Thalassiosira antarctica*	0.71	9
(Timmermans et al. 2007)	70	16:8	4.0	4.0	80	5	80	*Thalassiosira antarctica*	0.86	9
(Timmermans et al. 2007)	103	16:8	5.9	4.0	80	5	80	*Thalassiosira antarctica*	1.00	9
(Baumann et al. 1994)	4	24:0	0.3	-1.6	29	2	75	*Phaeocystis antartica*	0.20	10
(Baumann et al. 1994)	17	24:0	1.5	-1.6	29	2	75	*Phaeocystis antartica*	0.44	10

(Baumann et al. 1994)	51	24:0	4.4	-1.6	29	2	75	*Phaeocystis antartica*	0.65	10
(Baumann et al. 1994)	100	24:0	8.7	-1.6	29	2	75	*Phaeocystis antartica*	0.83	10
(Baumann et al. 1994)	161	24:0	13.9	-1.6	29	2	75	*Phaeocystis antartica*	0.95	10
(Baumann et al. 1994)	351	24:0	30.3	-1.6	29	2	75	*Phaeocystis antartica*	1.00	10
(Baumann et al. 1994)	5	24:0	0.4	1.0	29	2	75	*Phaeocystis antartica*	0.45	11
(Baumann et al. 1994)	19	24:0	1.6	1.0	29	2	75	*Phaeocystis antartica*	0.62	11
(Baumann et al. 1994)	52	24:0	4.5	1.0	29	2	75	*Phaeocystis antartica*	0.63	11
(Baumann et al. 1994)	101	24:0	8.7	1.0	29	2	75	*Phaeocystis antartica*	0.78	11
(Baumann et al. 1994)	161	24:0	13.9	1.0	29	2	75	*Phaeocystis antartica*	0.87	11
(Baumann et al. 1994)	353	24:0	30.5	1.0	29	2	75	*Phaeocystis antartica*	1.00	11
(Baumann et al. 1994)	4	24:0	0.3	-1.6	29	2	75	*Chaetoceros socialis*	0.13	12
(Baumann et al. 1994)	18	24:0	1.6	-1.6	29	2	75	*Chaetoceros socialis*	0.28	12
(Baumann et al. 1994)	50	24:0	4.3	-1.6	29	2	75	*Chaetoceros socialis*	0.43	12
(Baumann et al. 1994)	100	24:0	8.7	-1.6	29	2	75	*Chaetoceros socialis*	1.00	12
(Baumann et al. 1994)	160	24:0	13.8	-1.6	29	2	75	*Chaetoceros socialis*	0.50	12
(Baumann et al. 1994)	350	24:0	30.2	-1.6	29	2	75	*Chaetoceros socialis*	0.15	12

(Baumann et al. 1994)	5	24:0	0.4	1.0	29	2	75	*Chaetoceros socialis*	0.23	13
(Baumann et al. 1994)	19	24:0	1.7	1.0	29	2	75	*Chaetoceros socialis*	0.43	13
(Baumann et al. 1994)	52	24:0	4.5	1.0	29	2	75	*Chaetoceros socialis*	0.88	13
(Baumann et al. 1994)	101	24:0	8.8	1.0	29	2	75	*Chaetoceros socialis*	0.91	13
(Baumann et al. 1994)	162	24:0	14.0	1.0	29	2	75	*Chaetoceros socialis*	1.00	13
(Baumann et al. 1994)	352	24:0	30.4	1.0	29	2	75	*Chaetoceros socialis*	0.95	13
(Baumann et al. 1994)	3	24:0	0.3	-1.6	29	2	75	*Nitzschia curta*	0.16	14
(Baumann et al. 1994)	18	24:0	1.5	-1.6	29	2	75	*Nitzschia curta*	0.37	14
(Baumann et al. 1994)	50	24:0	4.4	-1.6	29	2	75	*Nitzschia curta*	1.00	14
(Baumann et al. 1994)	99	24:0	8.6	-1.6	29	2	75	*Nitzschia curta*	0.58	14
(Baumann et al. 1994)	160	24:0	13.8	-1.6	29	2	75	*Nitzschia curta*	0.37	14
(Baumann et al. 1994)	350	24:0	30.3	-1.6	29	2	75	*Nitzschia curta*	0.36	14
(Baumann et al. 1994)	5	24:0	0.4	1.0	29	2	75	*Nitzschia curta*	0.25	15
(Baumann et al. 1994)	18	24:0	1.6	1.0	29	2	75	*Nitzschia curta*	0.63	15
(Baumann et al. 1994)	51	24:0	4.4	1.0	29	2	75	*Nitzschia curta*	1.00	15
(Baumann et al. 1994)	100	24:0	8.6	1.0	29	2	75	*Nitzschia curta*	0.93	15

(Baumann et al. 1994)	159	24:0	13.8	1.0	29	2	75	*Nitzschia curta*	0.91	15
(Baumann et al. 1994)	350	24:0	30.2	1.0	29	2	75	*Nitzschia curta*	0.91	15
(Baumann et al. 1994)	4	24:0	0.4	-1.6	29	2	75	*Thalassiosira tumida*	0.00	16
(Baumann et al. 1994)	18	24:0	1.5	-1.6	29	2	75	*Thalassiosira tumida*	0.27	16
(Baumann et al. 1994)	52	24:0	4.5	-1.6	29	2	75	*Thalassiosira tumida*	0.74	16
(Baumann et al. 1994)	101	24:0	8.7	-1.6	29	2	75	*Thalassiosira tumida*	1.00	16
(Baumann et al. 1994)	160	24:0	13.8	-1.6	29	2	75	*Thalassiosira tumida*	0.94	16
(Baumann et al. 1994)	351	24:0	30.3	-1.6	29	2	75	*Thalassiosira tumida*	0.74	16
(Baumann et al. 1994)	4	24:0	0.3	1.0	29	2	75	*Thalassiosira tumida*	0.10	17
(Baumann et al. 1994)	18	24:0	1.5	1.0	29	2	75	*Thalassiosira tumida*	0.47	17
(Baumann et al. 1994)	50	24:0	4.3	1.0	29	2	75	*Thalassiosira tumida*	0.89	17
(Baumann et al. 1994)	100	24:0	8.7	1.0	29	2	75	*Thalassiosira tumida*	1.00	17
(Baumann et al. 1994)	160	24:0	13.8	1.0	29	2	75	*Thalassiosira tumida*	0.99	17
(Baumann et al. 1994)	351	24:0	30.4	1.0	29	2	75	*Thalassiosira tumida*	0.89	17

Table S3.

Sources of the required mean climatologies for salinity, temperature, dissolved oxygen, phosphate, silicate, nitrate, total alkalinity (TA), pCO_2, wind speed, and sea-ice concentration for the Southern Ocean south of 60°S. Daily mean climatologies were generated for sea-ice concentration, wind speed, temperature and salinity for calculations of air-sea gas exchange. Coarser, monthly mean climatologies were used for carbonate

parameters, as the spatiotemporal variability of these data has a small influence on CO_2 equilibration time-scales (Jones et al. 2014). Mean climatologies were bi-linearly interpolated along MOM01 particle trajectories (position saved every 5 days), without linear interpolation between months to avoid significant data loss due to sea-ice coverage.
WOA https://www.nodc.noaa.gov/OC5/woa18/woa18data.html
CCMP http://data.remss.com/ccmp/v02.0
NSIDC https://nsidc.org/data/seaice_index/archives
OISST https://www.ncdc.noaa.gov/oisst

Variable	Time period	Source	Resolution
surface salinity	All data	WOA (0-10m average) (Boyer et al. 2018)	1x1 degree, monthly
dissolved oxygen	All data	WOA (0-10m average) (Boyer et al. 2018)	1x1 degree, monthly
phosphate	All data	WOA (0-10m average) (Boyer et al. 2018)	1x1 degree, monthly
silicate	All data	WOA (0-10m average) (Boyer et al. 2018)	1x1 degree, monthly
nitrate	All data	WOA (0-10m average) (Boyer et al. 2018)	1x1 degree, monthly
temperature	2010-2018	NOAA OISST (Huang et al. 2021)	0.25x0.25 degree, daily
$pCO_{2\ sea}$	2010-2016	(Gregor et al. 2019)	1x1 degree, monthly
wind speed	2010-2018	CCMP reanalysis (Wentz et al. 2015)	0.25x0.25 degree, daily
sea-ice	2010-2018	NSIDC (Maslanik and Stroeve 1999)	25 km x 25 km, daily

Table S4. Export-ratios compiled for all available data from the Southern Ocean south of 60°S. Export-ratios were calculated as the ratio of particulate organic carbon (POC) flux at 100 m to net primary productivity (NPP) integrated over the euphotic zone. Flux data and locations were extracted from the given references. The applied method (Sediment trap or Thorium-based) is provided in the "Method" column. The NPP data were satellite-derived, using a 8 day climatology calculated with the CAFE algorithm (Silsbe et al. 2016) available at http://sites.science.oregonstate.edu/ocean.productivity/index.php. NPP values were spatially averaged over a 0.25 x 0.25° box centered on the location of flux measurements, and temporally averaged over 16 days in case of Thorium-based fluxes (^{234}Th residence time; (Henson et al. 2011)) or over the duration of trap deployments to better account for horizontal advection and export time-lags (Laws and Maiti 2019). Six export-ratios exceeding 1 (i.e. export flux > NPP) were removed from the analysis.

Reference	Latitude	Longitude	Date	Method	Export-ratio
(Asper and Smith 1999)	-77.1	173.1	23/11/94	Trap	0.179
(Asper and Smith 1999)	-76.6	173	6/12/94	Trap	0.088
(Asper and Smith 1999)	-76.5	172.9	18/11/94	Trap	0.054
(Asper and Smith 1999)	-76.5	171.8	24/12/95	Trap	0.180
(Asper and Smith 1999)	-76.5	170.8	27/12/95	Trap	0.148
(Asper and Smith 1999)	-76.5	165	2/1/96	Trap	0.160
(Asper and Smith 1999)	-76.5	177.6	7/1/96	Trap	0.177
(Asper and Smith 1999)	-76.5	165	12/1/96	Trap	0.166
(Cochran et al. 2000)	-76.5	-175.6	19/1/97	Thorium	0.204
(Cochran et al. 2000)	-76.5	-175.6	1/1/97	Thorium	0.707
(Cochran et al. 2000)	-76.5	-175.6	14/2/97	Thorium	0.294
(Cochran et al. 2000)	-76.5	165.8	13/1/97	Thorium	0.230
(Cochran et al. 2000)	-76.5	165.8	8/2/97	Thorium	0.962
(Cochran et al. 2000)	-76.5	165.8	18/2/97	Thorium	0.758
(Cochran et al. 2000)	-76.5	-175.6	19/1/97	Thorium	0.120

(Cochran et al. 2000)	-76.5	-175.6	1/2/97	Thorium	0.557
(Cochran et al. 2000)	-76.5	-165.8	13/1/97	Thorium	0.399
(Asper and Smith 1999)	-75	173	27/11/94	Trap	0.230
(Langone et al. 1997)	-74.7	175	13/12/94	Trap	0.007
(Langone et al. 1997)	-74	175	12/12/94	Trap	0.005
(Cochran et al. 2000)	-73.5	-175.4	24/1/97	Thorium	0.269
(Rodriguez y Baena et al. 2008)	-70.5667	-9.0333	20/12/03	Thorium	0.168
(Rodriguez y Baena et al. 2008)	-70.4667	-9.2	20/12/03	Thorium	0.051
(Rodriguez y Baena et al. 2008)	-70.3667	-9.3333	19/12/03	Thorium	0.025
(Rutgers van der Loeff et al. 2011)	-69.4	0	11/3/08	Thorium	0.240
(Rutgers van der Loeff et al. 2011)	-69.05	-17.35	15/3/08	Thorium	0.183
(Rutgers van der Loeff et al. 2011)	-69	-6.9	13/3/08	Thorium	0.109
(Rutgers van der Loeff et al. 2011)	-68.5	0	10/3/08	Thorium	0.081
(Buesseler et al. 2001)	-67.8	-170.1	17/1/98	Thorium	0.321
(Buesseler et al. 2003)	-67.8	-170	16/1/98	Thorium	0.357
(Shimmield et al. 1995)	-67.6	-84.9	7/12/92	Thorium	0.392
(Buesseler 1998)	-67.6	-84.9	15/11/92	Thorium	0.288
(Buesseler et al. 2001)	-67	-170	28/1/98	Thorium	0.347
(Buesseler et al. 2001)	-67	-170	15/2/98	Thorium	0.543
(Rutgers van der Loeff et al. 2011)	-66.93	-25.28	17/3/08	Thorium	0.160
(Rutgers van der Loeff et al. 2011)	-66.46	0	8/3/08	Thorium	0.123
(Buesseler et al. 2001)	-66.1	-168.7	28/2/98	Thorium	0.690

(Buesseler et al. 2003)	-66.1	-170	26/2/98	Thorium	0.713
(Buesseler et al. 2005)	-66	-172.5	29/1/02	Thorium	0.041
(Buesseler et al. 2005)	-66	-172.5	30/1/02	Thorium	0.082
(Buesseler et al. 2005)	-66	-172.5	3/2/02	Thorium	0.235
(Buesseler et al. 2005)	-66	-172.5	13/2/02	Thorium	0.304
(Buesseler et al. 2005)	-66	-172.5	19/2/02	Thorium	0.150
(Buesseler et al. 2005)	-66	-172.5	20/2/02	Thorium	0.376
(Rutgers van der Loeff et al. 2011)	-66	-32.76	20/3/08	Thorium	0.114
(Buesseler et al. 2001)	-65.2	-170.1	28/1/98	Thorium	0.903
(Buesseler et al. 2003)	-65.2	-170	27/1/98	Thorium	0.894
(Buesseler et al. 2001, 2003)	-65.167	-170.1	28/1/98	Thorium	0.903
(Rutgers van der Loeff et al. 2011)	-65.11	-40.31	22/3/08	Thorium	0.133
(Buesseler et al. 2001, 2003)	-64.833	-170.1	18/1/98	Thorium	0.597
(Buesseler et al. 2001)	-64.8	-170.1	18/1/98	Thorium	0.593
(Buesseler et al. 2003)	-64.8	-170	17/1/98	Thorium	0.694
(Rutgers van der Loeff et al. 2011)	-64.78	-42.88	23/3/08	Thorium	0.258
(Buesseler et al. 2001)	-64.7	-169.2	18/12/97	Thorium	0.302
(Buesseler et al. 2001)	-64.7	-169.3	8/3/98	Thorium	0.553
(Buesseler et al. 2001, 2003)	-64.7	-169.333	8/3/98	Thorium	0.556
(Buesseler et al. 2003)	-64.7	-170	17/12/97	Thorium	0.310
(Buesseler et al. 2003)	-64.7	-170	7/3/98	Thorium	0.557
(Buesseler et al. 2001, 2003)	-64.673	-169.186	18/12/97	Thorium	0.302
(Rutgers van der Loeff et al.	-64.48	0	28/2/08	Thorium	0.123

2011)					
(Buesseler et al. 2001)	-64.2	-169.2	16/12/97	Thorium	0.136
(Buesseler et al. 2003)	-64.2	-170	16/12/97	Thorium	0.122
(Buesseler et al. 2001, 2003)	-64.153	-169.186	16/12/97	Thorium	0.139
(Rutgers van der Loeff et al. 2011)	-64.03	-48.26	25/3/08	Thorium	0.155
(Buesseler et al. 2001)	-63.5	-170	25/12/97	Thorium	0.250
(Buesseler et al. 2001)	-63.5	-170	28/1/98	Thorium	0.533
(Buesseler et al. 2001)	-63.5	-170	15/2/98	Thorium	0.312
(Rutgers van der Loeff et al. 2011)	-63.46	-52.1	28/3/08	Thorium	0.280
(Le Moigne et al. 2016)	-63.45	-25.28	3/2/13	Thorium	0.210
(Rutgers van der Loeff et al. 2011)	-63.35	-52.85	29/3/08	Thorium	0.199
(Buesseler et al. 2001)	-63.1	-169.2	19/12/97	Thorium	0.288
(Buesseler et al. 2001)	-63.1	-169.9	24/2/98	Thorium	0.581
(Buesseler et al. 2003)	-63.1	-170	18/12/97	Thorium	0.293
(Buesseler et al. 2003)	-63.1	-170	23/2/98	Thorium	0.601
(Buesseler et al. 2001, 2003)	-63.087	-169.186	19/12/97	Thorium	0.288
(Buesseler et al. 2001, 2003)	-63.083	-169.883	24/2/98	Thorium	0.582
Charette unpublished	-62.553	-59.348	24/1/06	Thorium	0.097
(Buesseler et al. 2001)	-62.5	-170	4/11/97	Thorium	0.518
(Buesseler et al. 2003)	-62.4	-170	27/10/97	Thorium	0.587
(Buesseler et al. 2001, 2003)	-62.317	-170.003	28/10/97	Thorium	0.604
Charette unpublished	-62.254	-62.997	16/1/06	Thorium	0.241
Charette unpublished	-62.25	-58.002	24/1/06	Thorium	0.208

(Buesseler et al. 2001, 2003)	-62.033	-170.1	20/1/98	Thorium	0.532
(Buesseler et al. 2001)	-62	-170.1	20/1/98	Thorium	0.532
(Buesseler et al. 2001)	-62	-170.1	25/1/98	Thorium	0.278
(Buesseler et al. 2001, 2003)	-62	-170.1	25/1/98	Thorium	0.278
(Buesseler et al. 2003)	-62	-170	24/1/98	Thorium	0.262
(Buesseler et al. 2003)	-62	-170	19/1/98	Thorium	0.524
Charette unpublished	-61.999	-54.998	23/1/06	Thorium	0.190
Charette unpublished	-61.749	-59.029	19/1/06	Thorium	0.066
Charette unpublished	-61.748	-57.007	21/1/06	Thorium	0.290
Charette unpublished	-61.748	-55.752	22/1/06	Thorium	0.215
Charette unpublished	-61.747	-62	17/1/06	Thorium	0.646
(Buesseler et al. 2001)	-61.7	-168.8	14/12/97	Thorium	0.194
(Buesseler et al. 2001)	-61.7	-170.1	11/3/98	Thorium	0.185
(Buesseler et al. 2003)	-61.7	-170	13/12/97	Thorium	0.197
(Buesseler et al. 2003)	-61.7	-170	9/3/98	Thorium	0.177
(Buesseler et al. 2001, 2003)	-61.667	-168.833	14/12/97	Thorium	0.194
(Buesseler et al. 2001, 2003)	-61.667	-170.1	11/3/98	Thorium	0.185
Charette unpublished	-61.5	-60.491	18/1/06	Thorium	0.419
Charette unpublished	-61.5	-55.001	23/1/06	Thorium	0.152
Charette unpublished	-61.5	-54	23/1/06	Thorium	0.115
(Rutgers van der Loeff et al. 2011)	-61.48	0	27/2/08	Thorium	0.097
(Buesseler et al. 2001, 2003)	-60.917	-169.253	12/12/97	Thorium	0.415
(Buesseler et al. 2001)	-60.9	-169.3	12/12/97	Thorium	0.413

(Buesseler et al. 2003)	-60.9	-170	11/12/97	Thorium	0.420
(Buesseler et al. 2001)	-60.5	-169	1/11/97	Thorium	0.547
(Buesseler et al. 2001, 2003)	-60.5	-169	1/11/97	Thorium	0.548
(Buesseler et al. 2003)	-60.5	-170	31/10/97	Thorium	0.568
Charette unpublished	-60.261	-57.517	20/1/06	Thorium	0.123
Charette unpublished	-60.244	-57.01	21/1/06	Thorium	0.106
(Buesseler et al. 2001, 2003)	-60.233	-170.067	22/2/98	Thorium	0.478
(Buesseler et al. 2001, 2003)	-60.231	-170.071	10/12/97	Thorium	0.198
(Buesseler et al. 2001)	-60.2	-170.1	10/12/97	Thorium	0.198
(Buesseler et al. 2001)	-60.2	-170.1	22/2/98	Thorium	0.478
(Buesseler et al. 2003)	-60.2	-170	10/12/97	Thorium	0.194
(Buesseler et al. 2003)	-60.2	-170	20/2/98	Thorium	0.487
(Rutgers van der Loeff et al. 2011)	-60.1	-55.26	2/4/08	Thorium	0.490
(Buesseler et al. 2001)	-60	-170	4/11/97	Thorium	0.467
(Buesseler et al. 2001)	-60	-170	25/12/97	Thorium	0.274
(Buesseler et al. 2001)	-60	-170	15/2/98	Thorium	0.442
(Le Moigne et al. 2016)	-60	-29.48	5/2/13	Thorium	0.670

Table S5. All available b-values compiled for the Southern Ocean south of 60°S. All data that were available and accessible in the peer-reviewed literature were considered for the calculations of a b-value. b-values were calculated based on carbon fluxes from at least 3 depth levels by fitting the power-law function (Martin et al. 1987). Flux data were based on 3 different methods as indicated for each value (Sediment trap, Thorium-based, or estimated with underwater cameras (UVP)). We note that UVP-derived flux estimates have been validated before by Guidi et al. (2015), who found no statistical difference to thorium-derived flux estimates. All b-values are within a reasonable range

(Berelson 2001), except for one outlier (3.95 (i.e., very high rates of POC flux attenuation) from (Asper and Smith 1999)) which we removed from the analysis.

Reference	Latitude	Longitude	Date	Method	b-value
(Cochran et al. 2000)	-76.5	-178	2/11/96	Thorium	1.37
(Cochran et al. 2000)	-76.5	-178	19/1/97	Thorium	1.22
(Cochran et al. 2000)	-76.5	-178	1/2/97	Thorium	0.51
(Cochran et al. 2000)	-76.5	165.9	13/1/97	Thorium	0.47
(Cochran et al. 2000)	-76.5	165.9	8/2/97	Thorium	1.58
(Guidi et al. 2015)	-58.83	-21.25	20/10/95	UVP	1.26
(Guidi et al. 2015)	-58.83	-21.27	20/10/95	UVP	1.28
(Guidi et al. 2015)	-58.83	-21.22	20/10/95	UVP	1.37
(Guidi et al. 2015)	-58.67	-28.62	23/10/95	UVP	0.90
(Guidi et al. 2015)	-58.67	-31.17	24/10/95	UVP	0.95
(Guidi et al. 2015)	-58.67	-31.2	24/10/95	UVP	0.76
(Asper and Smith 1999)	-76.5	168.5	17/11/94	Trap	3.95
(Asper and Smith 1999)	-77.1	173.1	23/11/97	Trap	1.38
(Asper and Smith 1999)	-75	173	27/11/94	Trap	0.97
(Asper and Smith 1999)	-76.6	173	6/12/94	Trap	1.30
(Asper and Smith 1999)	-76.5	171.8	24/12/95	Trap	1.02
(Asper and Smith 1999)	-76.5	170.8	27/12/95	Trap	1.97
(Asper and Smith 1999)	-76.5	165	2/1/96	Trap	0.74
(Asper and Smith 1999)	-76.5	-177.6	7/1/96	Trap	0.72

(Asper and Smith 1999)	-76.5	165	21/1/96	Trap	0.56
(Buesseler et al. 2005)	-66.34	-171.96	30/1/02	Thorium	0.96
(Buesseler et al. 2005)	-66.34	-171.96	30/1/02	Thorium	1.10
(Buesseler et al. 2005)	-65.91	-170.79	19/2/02	Thorium	0.25
(Berelson 2001)	-61.5	-170	spring/summer (1997-1998)	Thorium, Trap	0.88
(Berelson 2001)	-65.5	-170	spring/summer (1997-1998)	Thorium, Trap	0.77
(Berelson 2001)	-68	-170	spring/summer (1997-1998)	Thorium, Trap	0.86
(Cavan et al. 2015)	-60.97	-48.14	3/2/13	MSC	1.51
(Cavan et al. 2015)	-60.97	-48.14	4/2/13	MSC	1.89
(Cavan et al. 2015)	-60.97	-48.14	5/2/13	MSC	1.03
(Shimmield et al. 1995)	-67.6	-84.93	7/12/92	Thorium	0.31
(Langone et al. 1997)	-74	175	12/12/94	Trap	0.70
(Langone et al. 1997)	-74.7	175	13/12/94	Trap	0.58

Table S6. Fertilization cost estimates of OIF ($US per km^2 of fertilized area) for different assumptions of fertilizer costs, daily ship costs, the distance to the OIF site, and the fraction of iron that becomes bioavailable (e.g., 0.8 means that 80% becomes bioavailable and 20% of the added Fe is lost due to inorganic particle sinking). The cost calculation equations are provided in the methods.

Fertilizer costs (US$ t^{-1})	Ship costs ($US d^{-1})	Inorganic particle sinking (fraction from 0-1)	Fertilization costs ($US km^{-2})
600	5000	0.2	101
600	5000	0.5	51
600	5000	0.8	39
600	7000	0.2	124
600	7000	0.5	65
600	7000	0.8	50
900	5000	0.2	121
900	5000	0.5	60
900	5000	0.8	44
900	7000	0.2	145
900	7000	0.5	74
900	7000	0.8	55

References

Alderkamp, A. C., G. L. Van Dijken, K. E. Lowry, and others. 2019. Effects of iron and light availability on phytoplankton photosynthetic properties in the Ross Sea. Mar. Ecol. Prog. Ser. **621**: 33–50. doi:10.3354/meps13000

Arrigo, K. R., M. M. Mills, L. R. Kropuenske, G. L. Van Dijken, A. C. Alderkamp, and D. H. Robinson. 2010. Photophysiology in two major southern ocean phytoplankton taxa: Photosynthesis and growth of phaeocystis antarctica and fragilariopsis cylindrus under different irradiance levels. Integr. Comp. Biol. **50**: 950–966. doi:10.1093/icb/icq021

Asper, V. L., and W. O. Smith. 1999. Particle fluxes during austral spring and summer in the southern Ross Sea, Antarctica. J. Geophys. Res. **104**: 5345–5359.

Baumann, M. E. M., F. P. Brandini, and R. Staubes. 1994. The influence of light and temperature on carbon-specific DMS release by cultures of Phaeocystis antarctica and three antarctic diatoms. Mar. Chem. **45**: 129–136. doi:10.1016/0304-4203(94)90097-3

Berelson, W. M. 2001. The Flux of Particulate Organic Carbon Into the Ocean Interior: A Comparison of Four U.S. JGOFS Regional Studies. Oceanography **14**: 59–67.

Bertrand, E. M., M. A. Saito, J. M. Rose, C. R. Riesselman, M. C. Lohan, A. E. Noble, P. A. Lee, and G. R. DiTullio. 2007. Vitamin B12 and iron colimitation of phytoplankton growth in the Ross Sea. Limnol. Oceanogr. **52**: 1079–1093. doi:10.4319/lo.2007.52.3.1079

Boyer, T., H. Garcia, R. Locarnini, and others. 2018. World Ocean Atlas 2018. NOAA National Centers for Environmental Information.

Buesseler, K. O. 1998. The decoupling of production and particulate export in the surface ocean. Global Biogeochem. Cycles **12**: 297–310.

Buesseler, K. O., J. E. Andrews, S. M. Pike, M. A. Charette, L. E. Goldson, M. A. Brzezinski, and V. P. Lance. 2005. Particle export during the Southern Ocean Iron Experiment (SOFeX). Limnol. Oceanogr. **50**: 311–327. doi:10.4319/lo.2005.50.1.0311

Buesseler, K. O., L. Ball, J. Andrews, J. K. Cochran, D. J. Hirschberg, M. P. Bacon, A. Fleer, and M. Brzezinski. 2001. Upper ocean export of particulate organic carbon and biogenic silica in the Southern Ocean along 170°W. Deep. Res. Part II Top. Stud. Oceanogr. **48**: 4275–4297. doi:10.1016/S0967-0645(01)00089-3

Buesseler, K. O., R. T. Barber, M. L. Dickson, M. R. Hiscock, J. K. Moore, and R. Sambrotto. 2003. The effect of marginal ice-edge dynamics on production and export in the Southern Ocean along 170°W. Deep. Res. Part II Top. Stud. Oceanogr. **50**: 579–603. doi:10.1016/S0967-0645(02)00585-4

Butterworth, B. J., and S. D. Miller. 2016. Air-sea exchange of carbon dioxide in the Southern Ocean and Antarctic marginal ice zone. Geophys. Res. Lett. **43**: 7223–

7230. doi:10.1002/2016GL069581

Campbell, J. W., and T. Aarup. 1989. Photosynthetically available radiation at high latitudes. Limnol. Oceanogr. **34**: 1490–1499. doi:10.4319/lo.1989.34.8.1490

Carter, B. R., R. A. Feely, N. L. Williams, A. G. Dickson, M. B. Fong, and Y. Takeshita. 2018. Updated methods for global locally interpolated estimation of alkalinity, pH, and nitrate. Limnol. Oceanogr. Methods **16**: 119–131. doi:10.1002/lom3.10232

Cavan, E. L., F. A. C. Le Moigne, A. J. Poulton, G. A. Tarling, P. Ward, C. J. Daniels, G. M. Fragoso, and R. J. Sanders. 2015. Attenuation of particulate organic carbon flux in the Scotia Sea, Southern Ocean, is controlled by zooplankton fecal pellets. Geophys. Res. Lett. **42**: 821–830. doi:10.1002/2014GL062744.Received

Coale, K. H., X. Wang, S. J. Tanner, and K. S. Johnson. 2003. Phytoplankton growth and biological response to iron and zinc addition in the Ross Sea and Antarctic Circumpolar Current along 170°W. Deep. Res. Part II Top. Stud. Oceanogr. **50**: 635–653. doi:10.1016/S0967-0645(02)00588-X

Cochran, J. K., K. O. Buesseler, M. P. Bacon, and others. 2000. Short-lived thorium isotopes (234Th, 228Th) as indicators of poc export and particle cycling in the ross sea, southern ocean. Deep. Res. Part II Top. Stud. Oceanogr. **47**: 3451–3490. doi:10.1016/S0967-0645(00)00075-8

Cullen, J. T., Z. Chase, K. H. Coale, S. E. Fitzwater, and R. M. Sherrell. 2003. Effect of iron limitation on the cadmium to phosphorus ratio of natural phytoplankton assemblages from the Southern Ocean. Limnol. Oceanogr. **48**: 1079–1087. doi:10.4319/lo.2003.48.3.1079

Eilers, P. H. C., and J. C. H. Peeters. 1988. A model for the relationship between light intensity and the rate of photosynthesis in phytoplankton. Ecol. Modell. **42**: 199–215. doi:10.1016/0304-3800(88)90057-9

Endo, H., H. Hattori, T. Mishima, G. Hashida, H. Sasaki, J. Nishioka, and K. Suzuki. 2017. Phytoplankton community responses to iron and CO2 enrichment in different biogeochemical regions of the Southern Ocean. Polar Biol. **40**: 2143–2159. doi:10.1007/s00300-017-2130-3

Gattuso, J.-P., J.-M. Epitalon, H. Lavigne, and J. Orr. 2021. Seacarb: seawater carbonate chemistry with R. R package version 3.0.

Gregor, L., A. D. Lebehot, S. Kok, and P. M. Scheel Monteiro. 2019. A comparative assessment of the uncertainties of global surface ocean CO2 estimates using a machine-learning ensemble (CSIR-ML6 version 2019a)-Have we hit the wall? Geosci. Model Dev. **12**: 5113–5136. doi:10.5194/gmd-12-5113-2019

Guidi, L., L. Legendre, G. Reygondeau, J. Uitz, L. Stemmann, and S. A. Henson. 2015. A new look at the ocean carbon remineralization for estimating deepwater sequestration. Global Biogeochem. Cycles **29**: 1044–1059. doi:10.1002/2014GB005063

366 Henson, S. A., R. Sanders, E. Madsen, P. J. Morris, F. Le Moigne, and G. D. Quartly.
367 2011. A reduced estimate of the strength of the ocean's biological carbon pump.
368 Geophys. Res. Lett. **38**: 10–14. doi:10.1029/2011GL046735

369 Holte, J., L. D. Talley, J. Gilson, and D. Roemmich. 2017. An Argo mixed layer
370 climatology and database. Geophys. Res. Lett. **44**: 5618–5626.
371 doi:10.1002/2017GL073426

372 Hopkinson, B. M., B. G. Mitchell, R. A. Reynolds, and others. 2007. Iron limitation across
373 chlorophyll gradients in the southern Drake Passage: Phytoplankton responses to
374 iron addition and photosynthetic indicators of iron stress. Limnol. Oceanogr. **52**:
375 2540–2554.

376 Huang, B., C. Liu, V. Banzon, E. Freeman, G. Graham, B. Hankins, T. Smith, and H. M.
377 Zhang. 2021. Improvements of the Daily Optimum Interpolation Sea Surface
378 Temperature (DOISST) Version 2.1. J. Clim. **34**: 2923–2939. doi:10.1175/JCLI-D-
379 20-0166.1

380 Jones, D. C., T. Ito, Y. Takano, and W. C. Hsu. 2014. Spatial and seasonal variability of
381 the air-sea equilibration timescale of carbon dioxide. Global Biogeochem. Cycles
382 **28**: 1163–1178. doi:10.1002/2014GB004813

383 Katlein, C., S. Arndt, H. J. Belter, G. Castellani, and M. Nicolaus. 2019. Seasonal
384 Evolution of Light Transmission Distributions Through Arctic Sea Ice. J. Geophys.
385 Res. Ocean. **124**: 5418–5435. doi:10.1029/2018JC014833

386 Kustka, A. B., B. M. Jones, M. Hatta, M. P. Field, and A. J. Milligan. 2015. The influence
387 of iron and siderophores on eukaryotic phytoplankton growth rates and community
388 composition in the Ross Sea. Mar. Chem. **173**: 195–207.
389 doi:10.1016/j.marchem.2014.12.002

390 Langone, L., M. Frignani, J. K. Cochran, and M. Ravaioli. 1997. Scavenging processes
391 and export fluxes close to a retreating seasonal ice margin (Ross Sea, Antarctica),
392 p. 705–715. *In* D. Evans, J. Wisniewski, and J. Wisniewski [eds.], The Interactions
393 Between Sediments and Water. Springer.

394 Laws, E. A., and K. Maiti. 2019. The relationship between primary production and export
395 production in the ocean: Effects of time lags and temporal variability. Deep Sea
396 Res. Part I Oceanogr. Res. Pap. doi:10.1016/j.dsr.2019.05.006

397 Van Leeuwe, M. A., R. Scharek, H. J. W. De Baar, J. T. M. De Jong, and L. Goeyens.
398 1997. Iron enrichment experiments in the Southern Ocean: Physiological responses
399 of plankton communities. Deep. Res. Part II Top. Stud. Oceanogr. **44**: 189–207.
400 doi:10.1016/S0967-0645(96)00069-0

401 Martin, J. H., G. a. Knauer, D. M. Karl, and W. W. Broenkow. 1987. VERTEX: carbon
402 cycling in the northeast Pacific. Deep Sea Res. Part A. Oceanogr. Res. Pap. **34**:
403 267–285. doi:10.1016/0198-0149(87)90086-0

404 Maslanik, J., and J. Stroeve. 1999. Near-Real-Time DMSP SSM/I-SSMIS Daily Polar
405 Gridded Sea Ice Concentrations.

406 Millero, F. J., T. B. Graham, F. Huang, H. Bustos-Serrano, and D. Pierrot. 2006.
407 Dissociation constants of carbonic acid in seawater as a function of salinity and
408 temperature. Mar. Chem. **100**: 80–94. doi:10.1016/j.marchem.2005.12.001

409 Mobley, C. D., and E. S. Boss. 2012. Improved irradiances for use in ocean heating,
410 primary production, and photo-oxidation calculations. Appl. Opt. **51**: 6549–6560.
411 doi:10.1364/AO.51.006549

412 Le Moigne, F. a. C., S. A. Henson, E. Cavan, and others. 2016. What causes the inverse
413 relationship between primary production and export efficiency in the Southern
414 Ocean? Geophys. Res. Lett. 4457–4466. doi:10.1002/2016GL068480

415 Öztürk, M., P. L. Croot, S. Bertilsson, K. Abrahamsson, B. Karlson, R. David, A.
416 Fransson, and E. Sakshaug. 2004. Iron enrichment and photoreduction of iron
417 under UV and PAR in the presence of hydroxycarboxylic acid: Implications for
418 phytoplankton growth in the Southern Ocean. Deep. Res. Part II Top. Stud.
419 Oceanogr. **51**: 2841–2856. doi:10.1016/j.dsr2.2000.10.001

420 Prytherch, J., I. Brooks, P. Crill, and others. 2017. Direct determination of the air-sea
421 CO2 gas transfer velocity in Arctic sea ice regions. Geophys. Res. Lett. **44**: 3770–
422 3778. doi:10.1002/2017GL073593

423 Rodriguez y Baena, A. M., R. Boudjenoun, S. W. Fowler, J. C. Miquel, P. Masqué, J. A.
424 Sanchez-Cabeza, and M. Warnau. 2008. 234Th-based carbon export during an ice-
425 edge bloom: Sea-ice algae as a likely bias in data interpretation. Earth Planet. Sci.
426 Lett. **269**: 596–604. doi:10.1016/j.epsl.2008.03.020

427 Rose, J. M., Y. Feng, G. R. Ditullio, and others. 2009. Synergistic effects of iron and
428 temperature on Antarctic phytoplankton and microzooplankton assemblages.
429 Biogeosciences **6**: 3131–3147. doi:10.5194/bg-6-3131-2009

430 Rutgers van der Loeff, M., P. H. Cai, I. Stimac, A. Bracher, R. Middag, M. B. Klunder,
431 and S. M. A. C. van Heuven. 2011. 234Th in surface waters: Distribution of particle
432 export flux across the Antarctic Circumpolar Current and in the Weddell Sea during
433 the GEOTRACES expedition ZERO and DRAKE. Deep. Res. Part II Top. Stud.
434 Oceanogr. **58**: 2749–2766. doi:10.1016/j.dsr2.2011.02.004

435 Sedwick, P. N., N. S. Garcia, S. F. Riseman, C. M. Marsay, and G. R. DiTullio. 2007.
436 Evidence for high iron requirements of colonial Phaeocystis antarctica at low
437 irradiance. Biogeochemistry **83**: 83–97. doi:10.1007/s10533-007-9081-7

438 Sedwick, P. N., G. R. Di Tullio, and D. J. Mackey. 2000. Iron and manganese in the
439 Ross Sea, Seasonal iron limitation in Antarctic. J. Geophys. Res. Ocean. **105**:
440 11321–11336. doi:10.1029/2000JC000256

441 Shimmield, G. B., G. D. Ritchie, and T. W. Fileman. 1995. The impact of marginal ice
442 zone processes on the distribution of 21OPb, 21OPo and 234Th and implications
443 for new production in the Bellingshausen Sea, Antarctica. Deep. Res. Part II **42**:
444 1313–1335. doi:10.1016/0967-0645(95)00071-W

445 Silsbe, G. M., M. J. Behrenfeld, K. H. Halsey, A. J. Milligan, and T. K. Westberry. 2016.

The CAFE model: A net production model for global ocean phytoplankton. Global Biogeochem. Cycles **30**: 1756–1777. doi:10.1002/2016GB005521

Strzepek, R. F., K. A. Hunter, R. D. Frew, P. J. Harrison, and P. W. Boyd. 2012. Iron-light interactions differ in Southern Ocean phytoplankton. Limnol. Oceanogr. **57**: 1182–1200. doi:10.4319/lo.2012.57.4.1182

Takeda, S. 1998. Influence of iron availability on nutrient consumption ratio. Nature **393**: 774–777.

Timmermans, K. R., M. A. Van Leeuwe, J. T. M. De Jong, and others. 1998. Iron stress in the Pacific region of the Southern Ocean: Evidence from enrichment bioassays. Mar. Ecol. Prog. Ser. **166**: 27–41. doi:10.3354/meps166027

Timmermans, K. R., M. J. W. Veldhuis, and C. P. D. Brussaard. 2007. Cell death in three marine diatom species in response to different irradiance levels, silicate, or iron concentrations. Aquat. Microb. Ecol. **46**: 253–261. doi:10.3354/ame046253

Venables, H., and C. M. Moore. 2010. Phytoplankton and light limitation in the Southern Ocean: Learning from high-nutrient, high-chlorophyll areas. J. Geophys. Res. **115**. doi:10.1029/2009jc005361

Viljoen, J. J., R. Philibert, N. Van Horsten, T. Mtshali, A. N. Roychoudhury, S. Thomalla, and S. Fietz. 2018. Phytoplankton response in growth, photophysiology and community structure to iron and light in the Polar Frontal Zone and Antarctic waters. Deep. Res. Part I Oceanogr. Res. Pap. **141**: 118–129. doi:10.1016/j.dsr.2018.09.006

Wanninkhof, R. 2014. Relationship between wind speed and gas exchange over the ocean revisited. Limnol. Oceanogr. Methods **12**: 351–362. doi:10.4319/lom.2014.12.351

Wentz, F. J., J. Scott, R. Hoffman, M. Leidner, R. Atlas, and J. Ardizzone. 2015. Remote sensing systems Cross-Calibrated Multi-Platform (CCMP) 6-hourly ocean vector wind analysis product on 0.25 deg grid, Version 2.0. Remote Sens. J.

Wu, M., J. S. P. McCain, E. Rowland, R. Middag, M. Sandgren, A. E. Allen, and E. M. Bertrand. 2019. Manganese and iron deficiency in Southern Ocean Phaeocystis antarctica populations revealed through taxon-specific protein indicators. Nat. Commun. **10**: 1–10. doi:10.1038/s41467-019-11426-z